Mechanism-Property Correlation in Coordination Polymer Crystals towards Design of Superior Sorbent

Cheng-Peng Li,[†,#] Hang Zhou,[†] Jia-Jun Wang,[†] Bo-Lan Liu,[†] Si Wang,[†] Xi Yang,[‡] Zhong-Liang Wang,[‡] Chun-Sen Liu,[§] Miao Du*[,†,§], and Wuzong Zhou*[,∥]

[†] College of Chemistry, Tianjin Key Laboratory of Structure and Performance for Functional Molecules, MOE Key Laboratory of Inorganic-Organic Hybrid Functional Material Chemistry, Tianjin Normal University, Tianjin 300387, P. R. China
[‡] Tianjin Key Laboratory of Water Resources and Environment, Tianjin Normal University, Tianjin 300387, P. R. China
[§] Henan Provincial Key Laboratory of Surface & Interface Science, Zhengzhou University of Light Industry, Zhengzhou 450002, P. R. China
[∥] School of Chemistry, University of St Andrews, St Andrews, Fife KY16 9ST, UK

KEYWORDS: coordination polymer; anion exchange; dichromate; perrhenate; superior sorbent; mechanism-property correlation.

ABSTRACT: A development of methodology for designing superior sorbents of oxoanions is performed. To integrate high efficiency of chemisorption, selectivity and recyclability into one sorbent, understanding the nature of oxoanions-sorbent interactions and the structural evolution of the sorbents is essential. Three cationic Ag(I) coordination polymers (CPs) are synthesized for dichromate ($Cr_2O_7^{2-}$) removal and three distinct oxoanion-exchange mechanisms are identified, namely the *replacement*, *breath*, and *reconstruction* processes, depending on degree of the framework distortion induced by the dichromate-CP interactions. The single-crystal to single-crystal transformation during the oxoanion-exchange has been investigated by using single-crystal X-ray diffraction, energy dispersive X-ray microanalysis. The *replacement* process due to a weak chemisorption shows excellent recyclability in cost of reduction of efficiency and selectivity of adsorption. The *reconstruction* process may achieve a high efficiency and selectivity, but it loses recyclability. Due to the formation of Ag–O(dichromate) bond and breathing effect of the framework, the sorbent with the *breath* mechanism shows both superior efficiency and high recyclability in dichromate removal. Study of perrhenate (ReO_4^-) removal using the same CPs demonstrates that one CP performing the *reconstruction* process in dichromate removal turns to the *breath* process in removal of perrhenate anions. These results of mechanism-property correlation provide an insight into improvement of the methodology to fabricate the most superior CP sorbent for oxoanion removal.

INTRODUCTION

Removal of trace contaminants from water is one of the important chemical separations in environmental science.[1] The ubiquitous presence of oxometal anionic pollutants has been considered as the serious issue to environment and human health.[2] Among all the treatment techniques for oxoanion removal from water streams, anion-exchange method holds considerable promise, given their ease of implementation.[3–5] As the important evaluation indexes, outstanding capture efficiency and recyclability seem to be incompatible within one sorbent. Chemisorption usually indicates fast sorption in kinetics and high capture in thermodynamics, because formation of the new chemical bonds ensures the superior stability of the products and largely promotes the anion-exchange reaction equilibrium. In comparison, physisorption or weak chemisorption shows remarkable recyclability during reversible sorption/desorption processes, which is more critical in industry manufacture. Is there any possibility to design a sorbent with both an efficient adsorption and a high recyclability? Until now, it still remains a challenge. Recent efforts have been made to focus on developing various oxoanion-exchange sorbents,[6–8] but lack of molecule-scale mechanism studies, which plays the key role to a new level of control over the capture efficiency and recyclability within one sorbent. It is well conceivable that, if a type of sorbent can be traced by molecule-scale mechanism analysis during the sorption process, this may enable us to estimate and optimize its anion-exchange performance. To explore the validity of above mentioned hypothesis, we were motivated by exploration of coordination polymers (CPs) for oxoanion removal and investigation of their mechanism-property correlation.

The porous materials of CPs are constructed from organic linkers and metal ions or clusters, and represent a promising class of crystalline materials with ordered networks, tunable pores, and satisfied physicochemical properties for practical applications.[9–11] Of further significance, comparing with other porous solids, one of the most unique features of CPs is that large crystals can be produced and their crystal structures can be unequivocally determined by single-crystal X-ray diffraction (SC-XRD) before and after the sorption process.[12,13] While numerous elegant examples of oxoanion-exchange by CPs are now known,[14] establishment of the oxoanion-exchange mechanisms is still at a primary stage. Up to date, the typical host-guest anion exchange equilibrium of physisorption or weak chemisorption is believed to play a dominant role to determine the trapping capacity and efficiency owing to the rigid host coordination frameworks.[15–17] Consequently, these oxoanion exchangers

possess good reversibility, but severe limitation in sorption efficiency.

As a matter of fact, another particular advantage of CPs, structure flexibility, has not be exploited in oxoanion removal yet. Given this property, the host frameworks can undergo various network distortions into new phases, to facilitate the formation of coordination interactions between the host framework and trapped target oxoanions. These newly formed coordination bonds are flexible due to the moderate bonding energy. Apparently, such chemisorption would affect the equilibrium of anion exchange thermodynamically and kinetically, thus enhancing the removal capacity and efficiency. With these in mind, we envision that there should exist three oxoanion-exchange mechanisms in CP crystals. The first is "*replacement* process", in which the CP framework undergoes very small change due to a physisorption or a weak chemisorption. The second is "*breath* process", in which the framework is heavily distorted due to the formation of coordination bonds between trapped oxoanions and the framework. However, the coordination bonds are not strong enough to break any bonds in the framework. The flexible coordination bonds between the oxoanions and the frameworks endow the CPs with great potential to surmount the paradoxical issues of efficiency and recyclability. During the reversible adsorption/desorption, the framework undergoes a breathing-like distortion-recovery-distortion process. The third is "*reconstruction* process", in which the chemisorption is so strong that the original framework is broken, transforming to a new structure (Figure 1).

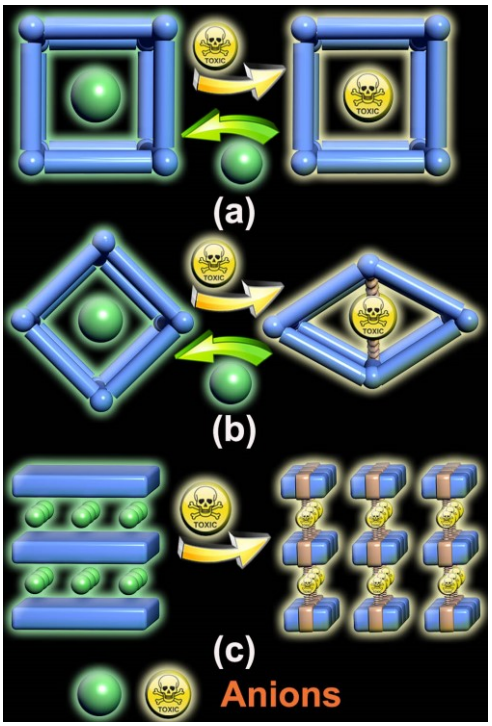

Figure 1. Schematic view of the three distinct oxoanion-exchange mechanisms of coordination polymers. (a) "*Replacement* process". It provides a void channel for oxoanion exchange in a reversible way with the framework almost intact. (b) "*Breath* process". It shows flexible pores upon oxoanion trapping/releasing. (c) "*Reconstruction* process". The crystalline framework undergoes a drastic reconstruction.

To explore the validity of this hypothesis, we chose three homologous tripyridyltriazole ligands as shown in Figure S1 of Supporting Information (SI) and Ag(I) as building units to produce three new cationic CPs, designated TJNU-244, TJNU-243, and TJNU-334 (TJNU-CPs in general. TJNU denotes Tianjin Normal University). To demonstrate the proof of concept, dichromate anion was employed as target oxoanion, given its top-prior toxic nature.[18,19] With the aid of SC-XRD, the three different oxoanion-exchange mechanisms are proposed at molecular level via single-crystal to single-crystal (SC-SC) transformations. The distinct mechanisms govern the different dichromate removal behaviors of TJNU-CPs. In detail, TJNU-244 follows the common *replacement* mechanism, and thus possesses recyclability of dichromate adsorption. Based on the *reconstruction* process, TJNU-334 shows good uptake efficiency. As for TJNU-243, the *breath* process endows it with the advantages of TJNU-244 and TJNU-334, including relatively superior properties in the adsorption capacity, kinetics, selectivity, removal ability at very low concentrations of dichromate, and good recyclability. Therefore, the mechanism-property correlation for fabricating superior sorbents can be established. In order to further valid its universality, we chose perrhenate (ReO_4^-) as another target oxoanion, which is a structural surrogate of pertechnetate ($^{99}TcO_4^-$), a troublesome radioactive waste and urgent threat to the international community.[20-23] As a result, both TJNU-334 and TJNU-243 following the *breath* process, show more advantages than TJNU-244, which follows the *replacement* process, coinciding with the mechanism-property correlation.

EXPERIMENTAL SECTION

The three tripyridyltriazole ligands, 3-(2-pyridyl)-4,5-bis(4-pyridyl)-1,2,4-triazole (L^{244}), 3-(2-pyridyl)-4-(4-pyridyl)-5-(3-pyridyl)-1,2,4-triazole (L^{243}) and 3,4-bis(3-pyridyl)-5-(4-pyridyl)-1,2,4-triazole (L^{334}) were synthesized according to the literature method.[24] All other chemicals and solvents were obtained commercially and used as received without further purification. The following paragraphs highlight the conditions of synthesis, anion exchange and characterization methods. More detailed information of the experiments is given in Supporting Information.

Synthesis of TJNU-CPs. An organic solution (methanol for L^{244} and L^{334}, acetonitrile for L^{243}) of ligand (0.1 mmol) was carefully layered onto a buffer of ethyl acetate in a straight glass tube, below which a 0.1 mmol Ag^+ solution (aqueous solution of $AgNO_3$ for TJNU-244 and TJNU-243, dimethylformamide solution of $AgBF_4$ for TJNU-334) was pre-filled. The tube was left to stand at room temperature in darkness for three to five days. Colorless block crystals of TJNU-CPs were found on the tube wall.

Single-Crystal to Single-Crystal Transformations. Single crystals of TJNU-CPs were dipped in an aqueous solution (5 mL) of 1 μM $K_2Cr_2O_7$ or $KReO_4$ for 24 to 48 h at ambient conditions, affording good-quality single-crystals of the anion-exchanged products.

Anion Exchange Procedure. The as-synthesized TJNU-CPs (0.2 or 0.1 mmol) were immersed in an aqueous solution of $K_2Cr_2O_7$ or $KReO_4$ (0.1 mmol), which was mildly stirred at room temperature. The exchange progress was monitored at different time intervals by UV-vis spectra or ICP-MS measurement. Anion removal from dilute solutions was also performed by immersing 0.1 mmol TJNU-CPs in a dilute aqueous solution

of $K_2Cr_2O_7$ or $KReO_4$ (10 mg L^{-1} to 50 μg L^{-1}, 10 mL) under mild stirring for one to three days.

Reversibility of Anion Exchange. The dichromate-adsorbed sample, 0.1 mmol TJNU-CP(Cr) or TJNU-CP(Re), was dipped in a 1 M $NaNO_3$ aqueous solution (5 mL) under mild stirring for one day. The crystalline sample was characterized using powder X-ray diffraction (PXRD) and Fourier transform Infrared (FT-IR) spectroscopy. The desorbed sample was used for adsorption again.

Characterization Methods. The crystalline phases of the samples were initially checked by PXRD on Bruker D8 Advance diffractometer. Simulation of the PXRD patterns was performed based on the single-crystal data using diffraction-crystal module of Mercury (Hg) program. The crystal structures of the samples were determined by analysis of the SC-XRD data, collected on a Bruker Apex II CCD diffractometer with graphite-monochromated Mo-Kα radiation (λ = 0.71073 Å) as well as on an Agilent SuperNova diffractometer with graphite-monochromated Cu-Kα radiation (λ = 1.54178 Å).

FT-IR spectra in a range of 4000–400 cm^{-1} were recorded on a Bruker Tensor 27 OPUS FT-IR spectrometer (with KBr pellets). Elemental analyses of C, H, and N were performed on a CE-440 (Leemanlabs) analyzer. Thermogravimetric analysis (TGA) data were recorded on a Shimadzu DTG-60A thermal analysis instrument from room temperature to 800 °C with a heating speed of 10 °C min^{-1}. UV-vis absorption spectra were taken on a PerkinElmer Lambda 35 spectrophotometer. Inductively coupled plasma mass spectrometry (ICP-MS) analysis was performed on an Ultima2 spectrometer. Scanning electron microscopy (SEM) and energy-dispersive X-ray spectroscopy (EDS) were performed on a FEI Nova Nano 230 scanning electron microscope, with the energy of the electron beam of 15 or 20 keV.

RESULTS AND DISCUSSION

Oxoanion-Exchange of TJNU-CPs

Replacement* Process.** This mechanism represents a common host-guest anion exchange equilibrium of physisorption or weak chemisorption, which can be clearly demonstrated by comparing the crystal structures of TJNU-244 and oxoanion-exchanged product, TJNU-244(Cr). SC-XRD analysis of TJNU-244 shows that it has a 3D cationic coordination framework (Figure 2a). The framework has a monoclinic unit cell with a = 10.0017(15), b = 14.488(2), c = 15.422(3) Å, and β = 104.400(3)° (Part 1, Table S1). There are uniform one dimensional (1D) channels along the crystallographic ***a axis, with the pore dimensions of 11.92 × 10.01 $Å^2$ (diagonal Ag···Ag distances by considering the van der Waals radius of Ag atoms, similarly hereinafter), which accommodate nitrate anions and can be accessible for anion exchange (Figure S2).

The crystal structure of TJNU-244(Cr) after oxoanion exchange is also monoclinic with a = 9.6747(12), b = 14.9827(18), c = 14.770(2) Å, and β = 106.674(14)°. The structure is similar to that of TJNU-244 with small changes of the unit cell dimensions by –3%a, +3%b, –4%c and +2%β. The unit cell volume reduces by ca. 5% (Tables S1 and S2). The oxoanion-exchange process in TJNU-244 (Figure 2a) with a simple replacement of NO_3^- by $Cr_2O_7^{2-}$ makes a very small distortion in the CP framework. The process is therefore designated "*replacement* process". Based on the SC-XRD analysis, the dichromate oxoanions form C–H···O bonds with the host framework (H···O bond length: 2.45 and 2.49 Å), which can be regarded as a weak chemisorption. Moreover, due to the positive-charged

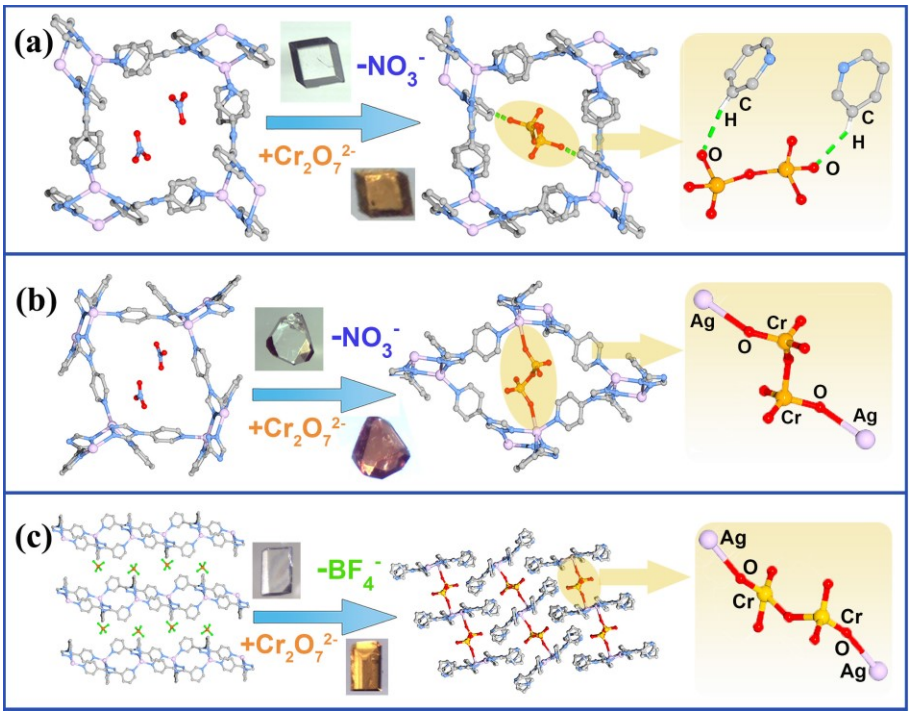

Figure 2. Three distinct dichromate removal processes by TJNU-CPs via SC-SC transformations, showing (from left to right) TJNU-CP, TJNU-CP(Cr) and bonding between dichromate anion with the CP framework. (a) TJNU-244 in the *replacement* process. (b) TJNU-243 in the *breath* process. (c) TJNU-334 in the *reconstruction* process. The photographs show colour changes of the crystals before (left) and after (right) the anion exchange.

framework of TJNU-244, the electrostatic interaction plays a cooperative role to promote the adsorption process.

***Breath* Process.** With regard to this mechanism, the framework of TJNU-243 undergoes a significant distortion during the anion exchange of dichromate, but no destruction taking place in the framework. The structure of TJNU-243 with

a formula of $C_{19}H_{17}N_8O_4Ag$ is monoclinic with a = 10.451(6), b = 14.546(8), c = 15.362(7) Å, and β = 116.00(3)° (Part 2, Table S1). As shown in Figures 2b and S3, its 3D network possesses the uniform 1D channels along the crystallographic ***a*** axis, with the pore dimensions of 11.58 × 10.82 $Å^2$ for accommodating nitrate anions.

After a complete exchange of nitrate by dichromate anions, the structure of TJNU-243(Cr) is still monoclinic with a large change of the unit cell parameters, a = 9.5768(7), b = 18.3357(13), c = 10.6982(8) Å, and β = 107.712(2)° as determined by SC-XRD (Part 2, Table S1). The unit cell of TJNU-243(Cr) is derived from that of the original TJNU-243 by large changes of the parameters, –8.3%*a*, +26%*b*, –30%*c*, and –7.1%β. The unit cell volume changes by –14.7% (Tables S1 and S2). In comparison with TJNU-244(Cr), lattice distortion in TJNU-243(Cr) is much more significant. Different from that observed in TJNU-244, the Ag–O coordination bond (2.577 Å) is newly formed in TJNU-243(Cr). As a result, the opposite corners of 1D channels are connected by the dichromate anions and the channel shape is distorted from pseudo-square to rhombic (Figure 2b). The pore dimensions become 12.69 × 5.82 $Å^2$ (Figure S4). It is a good example showing that the trapped dichromate anions afford strong coordination interactions with the adsorbent and remodel the interior pore shapes, as directly and accurately pictured by the SC-XRD technique.[25] The original TJNU-243 framework can be recovered when the adsorbed dichromate anions are substituted by nitrate anions in a reversed process. To take account of reversible distortion of the pores in the framework, this oxoanion exchange process is therefore named "*breath* process".

***Reconstruction* Process.** It is complicated that the CP framework could be broken into numerous components during the oxoanion-exchange, which undergo local rotation/shift to self-rearrange into a new structure In TJNU-334 of a formula of $C_{23}H_{26}BF_4N_8O_2Ag$, the structure is monoclinic with a = 17.181(9), b = 8.894(5), c = 18.218(9) Å, and β = 99.351(9)° (Part 3, Table S1). Ag(I) atoms are connected by the L^{334} ligands to form 2D layers (Figure S5). As shown in Figure 2c, the lattice tetrafluoroborate anions are located in the interlayer space.

Given that TJNU-334 contains highly charged cationic layers, we predict that the anion exchange of tetrafluoroborate by dichromate will proceed within the interlayer voids. However, significant variations in the structure can be found according to the SC-XRD result of TJNU-334(Cr). It is monoclinic with the unit cell parameters, a = 9.4255(8), b = 20.3962(16), c = 10.4230(8) Å, and β = 108.198(2)° (Part 3, Table S1). Similarity in the unit cell dimensions can be hardly found between TJNU-334(Cr) and its parent compound TJNU-334 (Tables S1 and S2). In TJNU-334(Cr), the L^{334} molecules act as tridentate ligands to connect three Ag(I) centers to form a 1D Ag–L^{334} chain motif (Figure S6b). The dichromate anions interconnect the neighboring 1D chains into a 2D layer (Figures 2c and S6c). Obviously, the coordination network of TJNU-334 undergoes a more complicated bond breakage and re-connection process, leading to a new structure of TJNU-334(Cr). This phase transformation is not reversible and therefore designated "*reconstruction* process".

Periodic Boundary Calculation. Periodic boundary calculations of each compound were carried out with density functional theory within the projected-augmented plane wave method as implemented in Vienna ab initio simulation package (VASP) (for more details, see SI).[26] The ground state energies (in eV) of the compounds were obtained as TJNU-244 (–1091.52) and TJNU-244(Cr) (–1170.71); TJNU-243 (–1092.26) and TJNU-243(Cr) (–1179.76); TJNU-334 (–1107.72) and TJNU-334(Cr) (–1231.23). The energy difference of adsorbents before and after the adsorption of $Cr_2O_7^{2-}$ anions are 79.19, 87.5, and 123.51 eV, respectively. The significantly large energy difference of TJNU-334 and TJNU-334(Cr) associates with the relatively stronger framework-oxoanion bonding and the big structural change.

Domain Structure. Bearing in mind that the overall crystal shapes did not change during the anion exchange even the starting and end crystal structures were very different, the microstructures of some intermediate phases of the phase transformation have been investigated in order to understand the structural evolution. Typical SC-XRD patterns from TJNU-CPs with nitrate or tetrafluoroborate only partly replaced by dichromate with exchange time of 6 h were recorded. The SC-XRD patterns from TJNU-244 and TJNU-243 are polycrystalline patterns (Figures S7a, b). EDS elemental mapping of a crystal of TJNU-244(NO_3^-, $Cr_2O_7^{2-}$) shows that the Cr distribution in the crystal is not even. The near surface area is Cr rich and some small Cr rich regions are also found in the central area of the crystal (Figure 3a), indicating a domain structure. A similar result is seen from TJNU-243(NO_3^-, $Cr_2O_7^{2-}$) (Figure 3b). Figure 4 shows a schematic drawing of the phase transformation via domain structures during dichromate adsorption in TJNU-244 and TJNU-243. The shape of the crystals would not change.

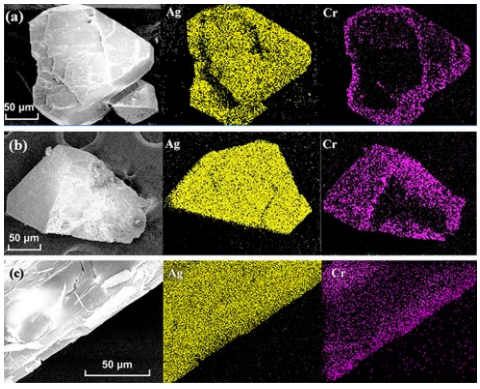

Figure 3. SEM image of a single crystal and the corresponding elemental mapping of Ag and Cr, (a) TJNU-244, (b) TJNU-243 and (c) TJNU-334 with NO_3^-/BF_4^- partly replaced by $Cr_2O_7^{2-}$.

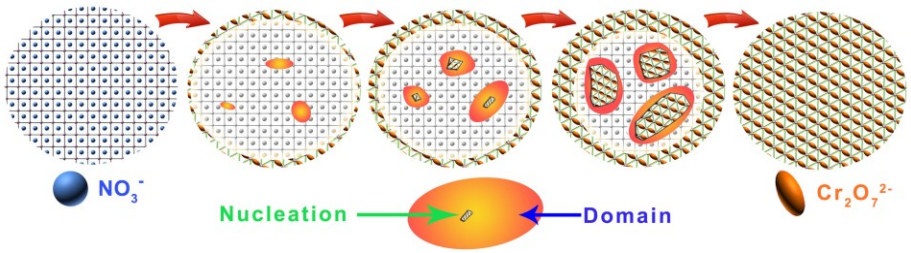

Figure 4. Schematic drawing of dichromate adsorption mechanism via domain structures in TJNU-244 and TJNU-243.

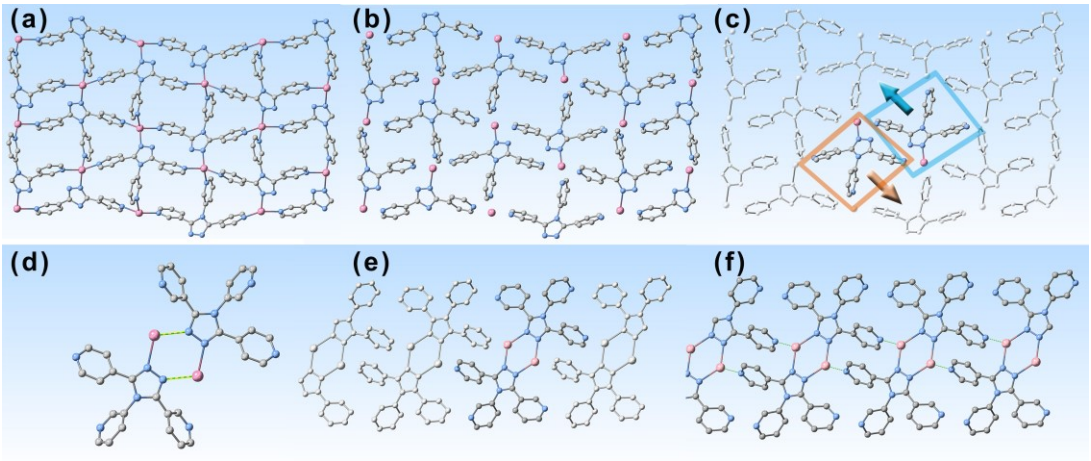

Figure 5. Hypothesis on the structural transformation from TJNU-334 to TJNU-334(Cr). (a) The original 2D sheet in TJNU-334. (b) The sheet undergoes breakage of all the coordination bonds of Ag–N_{py} into L^{334}–Ag monomers, induced by invasion of dichromate anions. (c) Shift of the monomers, leading to a new connection of the monomers. (d) Formation of $(L^{334}–Ag)_2$ dimer through double N_{tri}–Ag–N_{tri} bridges. (e) 1D arrangement of the dimers. (f) Formation of 1D chain motif via Ag–N_{py} bonds.

Domain structures are often observed in mixed metal oxide crystals due to local lattice distortion. For example, in Nb-doped Bi_2O_3 solid solution crystals, Nb^{5+} cations prefer to have a different coordination of oxygen from that of Bi^{3+} cations and form Nb-rich clusters in the Bi_2O_3 matrix. This is because when a Nb^{5+} cation replaces a Bi^{3+}cation, the local structure is distorted and become more suitable to accept other Nb^{5+} cations. It is the so-called "like with like" phenomenon.[27,28] In this case, a random distribution of Nb^{5+} cations is difficult. The same principle can be applied to TJNU-CPs. When a dichromate anion replaces two nitrate anions at one site, the neighboring crystal lattice is distorted, becoming more suitable to accommodate other dichromate anions. Some Cr-rich clusters or domains would form. As these domains grow larger, nucleation and crystal growth of the secondary phase, TJNU-CP(Cr), take place. At an intermediate stage, the crystals become polycrystalline containing both the TJNU-CP and TJNU-CP(Cr) components (Figure 4).

SC-XRD pattern of an intermediate phase of TJNU-334 with partial oxoanion exchange shows very low crystallinity (Figure S7c), indicating decomposition of a large part of the crystal, although the shape of the crystals still maintains. EDS elemental mapping shows relatively even distribution of Cr without obvious domain structure (Figure 3c). This is because the interlayer space occupied by tetrafluoroborate anions in TJNU-334 is much smaller than the channels in other two CPs. The invasion of dichromate anions introduces very large lattice tension, leading to breakage of some chemical bonds. The lattice distortion associated to the substitution of dichromate anions would be released by the bond breaking and would not extend to the neighboring sites to generate a larger suitable environment for the formation of Cr-rich clusters. A polymorphic and intricate structural transformation takes place inside the crystal, resulting in a significant structural change from TJNU-334 to TJNU-334(Cr).

To elucidate the principle of the phase transformation in TJNU-334, Figure 5 shows a schematic drawing of the most important steps of the structural changes during the oxoanion exchange. The 2D polymeric sheets consist of L^{334}–Ag monomers connected each other with coordination bonds of Ag–N_{py} (py: pyridyl) (Figure 5a). When $Cr_2O_7^{2-}$ are inserted, very large lattice tension breaks the Ag–N_{py} bonds, turning the 2D sheet into separated monomers (Figure 5b). Each $Cr_2O_7^{2-}$ anion is sandwiched by two monomers in two adjacent layers. The monomers can shift in the layers (Figure 5c) and form $(L^{334}–Ag)_2$ dimers with double N_{tri}–Ag–N_{tri} (tri: triazole) bridges (Figure 5d). These dimers are interconnected with the Ag–N_{py} bonds to construct 1D chain motif (Figures 5e, f). Since all Ag(I) cations locate in the middle of the chains and the edges of the chains are Ag-free, construction of 2D sheets by the new building units is not possible. In a real process, before the formation of the chain structures, the monomers may lose their ordering and orientation, thus giving a poor crystallinity as shown by the SC-XRD pattern (Figure S7c).

Mechanism-Property Correlation. Based on the results above, we can now formulate three oxoanion-exchange mechanisms of TJNU-CP crystals. Given the fact that known oxoanion exchange often follows the *replacement* and

reconstruction mechanisms, we expect that the *breath* mechanism with both high efficiency and elegant recyclability will be of high relevance for practical anion-exchange processes. In TJNU-243, the tunable Ag–O bonding and flexible framework endow it with breathing capability, to display high potentials of chemical sorption and desorption during oxoanion-exchange. With these in mind, the performance of TJNU-CPs in dichromate removal was investigated.

Sorption Isotherms. Anion exchange of dichromate was explored by immersing 0.2 mmol TJNU-CP into a 10 mL aqueous solution containing 0.1 mmol $K_2Cr_2O_7$. The results indicate that the equilibrium adsorption time of dichromate appears to follow the order of TJNU-243 < TJNU-334 < TJNU-244, varying from 8 to 30 h (Figure 6a). It conforms to the fact that, TJNU-243 and TJNU-334 undergo relatively strong chemical processes of oxoanion-exchange and TJNU-244 shows a weaker chemisorption. Exchange capacities up to 269, 273, and 293 mg of dichromate per gram of TJNU-CPs were observed for TJNU-244, TJNU-243, and TJNU-334, respectively, which are close to the theoretical values of the maximum adsorption in these CPs. In this condition, these TJNU-CPs do not display obvious differences in the removal percentage (>98%), possibly due to their similar capture ability in the high concentration of dichromate.

The kinetic studies illustrate that the exchange of $Cr_2O_7^{2-}$ in TJNU-CPs can be better described as pseudo-second-order kinetics (Figure S8). In view of such a process, chemisorption might be crucial in the rate-controlling step. The rate constant (k) and the initial sorption rate (h) for exchange of $Cr_2O_7^{2-}$ into TJNU-CPs at 298 K follow the order of TJNU-243 > TJNU-334 > TJNU-244, with the k values of 2.816×10^{-3}, 8.868×10^{-4}, 3.991×10^{-4} g mg^{-1} min^{-1}, and the h values of 200.8, 75.59, 28.46 mg g^{-1} min^{-1}, respectively (Table S3). At this stage, the higher kinetic parameters of TJNU-243 and TJNU-334 suggest that there are chemical bonds with moderate strength in the final products.

Sorption in Lower Concentration. It is feasible to evaluate the anion sorption ability of TJNU-CPs with different mechanisms in lower concentration solution of dichromate. As defined by the US Environmental Protection Agency (EPA), the allowed maximum contaminant level of Cr(IV) is 0.05 mg L^{-1} for drinking water.[29] As an initial test of very dilute solution, the anion exchanges in different concentration ranges (10 mg L^{-1}, 5 mg L^{-1}, 1 mg L^{-1}, 500 μg L^{-1}, 100 μg L^{-1} and 50 μg L^{-1}) were performed and monitored using ICP-MS. As shown in Figure 6b, the TJNU-CPs have very high capability of dichromate removal (86–99%) at such low concentrations and the lowest residual concentration of dichromate is only 1 μg L^{-1} (adsorbent: TJNU-243, original concentration of $K_2Cr_2O_7$: 50 μg L^{-1}). In comparison of these three materials, TJNU-243 shows significantly higher anion exchange capabilities than TJNU-244 at the mg L^{-1}/μg L^{-1} levels, which can also be attributed to its potential to form relatively stronger chemical bonding with the dichromate anions. This feature makes it the most attractive candidate for removal of trace dichromate contaminants from waste water.

Selectivity. Removal selectivity is also a characteristic to demonstrate the different mechanisms of dichromate adsorption. To confirm their selectivity for dichromate capture, an as-synthesized TJNU-CP sample (0.1 mmol) was immersed in a solution (10 mL) of $K_2Cr_2O_7$ (0.1 mmol) coexisting with another type of anions of a high concentration, e.g. $CH_3CO_2^-$, SO_4^{2-}, NO_3^-, BF_4^-, $CF_3CO_2^-$ or $CH_3SO_3^-$ at room temperature for two days. FT-IR and PXRD results (Figure S9) of the products after anion exchange indicate that, TJNU-334 and TJNU-243 show higher selectivities than TJNU-244 (Figure 6c) towards most secondary anions ($CH_3CO_2^-$, NO_3^-, BF_4^-, and $CF_3CO_2^-$). It can be attributed to the relatively weaker interaction between the framework of TJNU-244 and dichromate anions.

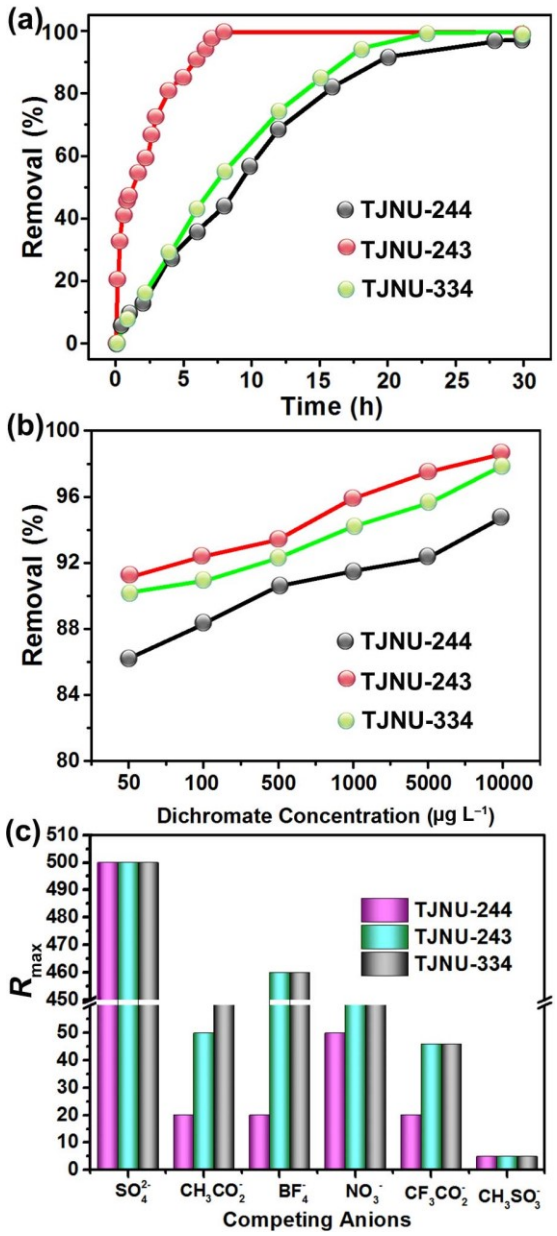

Figure 6 (a) Sorption isotherms for TJNU-CPs, showing the adsorption curves of dichromate exchange capacities versus contact time in an aqueous solution. (b) Removal percentage of dichromate in the dilute solutions from 50 μg L^{-1} to 10 mg L^{-1}. (c) The highest ratios of the competing anions to $Cr_2O_7^{2-}$, R_{max}, when the adsorption of the former was not detectable.

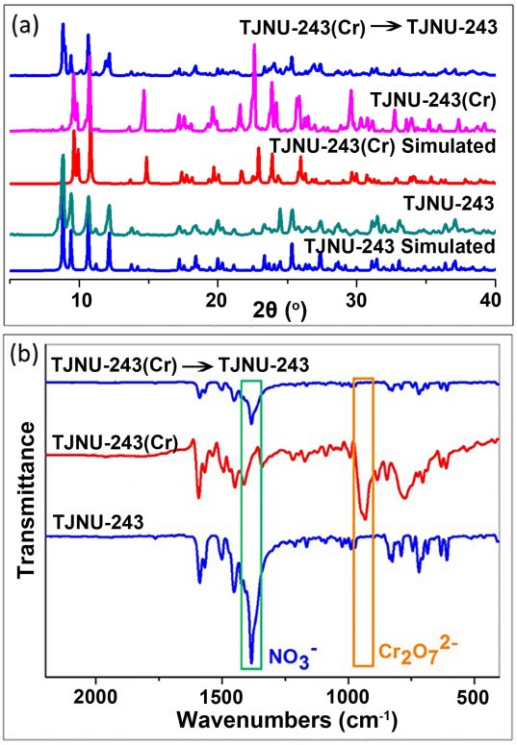

Figure 7. (a) PXRD patterns and (b) FT-IR spectra of TJNU-243 in a full trapping-releasing process of dichromate anion exchange, showing a high reversibility.

Reversibility and Stability. Following the *replacement* mechanism during the reversible process, the dichromate anions in TJNU-244(Cr) can be easily re-exchanged by nitrate anions at room temperature. The crystals transform back to pure nitrate-containing TJNU-244 (Figures S10 and S11). Obviously, this reversibility of oxoanion exchange is due to the weak hydrogen bonds between the framework and oxoanion in TJNU-244(Cr). While for TJNU-334, re-exchange of dichromate requires a very high energy to change the TJNU-334(Cr) structure back to the original framework. Regarding TJNU-243, though the framework is distorted when dichromate anions are adsorbed, it is well conceivable that elaborate tuning on desorption condition may break the Ag–O bonds and the original framework is recovered. As a test, immersing TJNU-243(Cr) into a solution of $NaNO_3$ (1 M) and heating to 50 °C, the orange-colored crystals turned opaque, indicating loss of its single-crystallinity. Determined by FT-IR and PXRD (Figure 7), the desorption product is TJNU-243. Consequently, the sorbent following the *breath* mechanism is readily to show good recyclability (Figure S12).

For oxoanion removal, the stability of the sorbent materials is extremely important. Therefore, the behaviors of TJNU-CPs and TJNU-CPs(Cr) in aqueous solution with different pH values and their thermal stabilities were tested. All of the materials kept stable in weak acid, neutral, and weak base conditions (Figure S13). In detail, TJNU-244, TJNU-243, and TJNU-334 can maintain their frameworks in the aqueous solution of pH = 4–11, 2–12, and 3–11, respectively. The slight differences may due to their different molecule structures. Their dichromate-exchanged counterparts are stable in the pH ranges of 4–11, 4–10, and 4–10, in which the range changes may be ascribed to the vulnerable Ag–O(dichromate) bonds in acid or base conditions. Thermal stability of the TJNU-CPs and TJNU-CPs(Cr) was explored by TGA experiments (Figure S14). The host frameworks of TJNU-244, TJNU-243, and TJNU-334 can keep stable up to ca. 272, 245, and 241 °C. After oxoanion exchange, the values changed to 220, 224, and 216 °C, all of which showed decreasing trend.

Oxoanion Exchange of Perrhenate. The bonding ability of dichromate to the TJNU-CPs frameworks plays a key role in sorption mechanisms. It implies that the mechanism depends not only on the adsorbent, but also on the adsorbate. This result prompts us to evaluate another oxoanion, perrhenate (ReO_4^-), which has a tetrahedral geometry and low electron density. Therefore, perrhenate shows weaker coordination ability than dichromate. With this in mind, we surmise that the *reconstruction* mechanism might be avoided. To verify this hypothesis, TJNU-CPs crystals were immersed into a water solution (20 mL) containing 0.1 mmol $KReO_4$. Interestingly, these oxoanion exchange processes are accompanied by SC-SC transformations, to afford TJNU-CPs(Re) crystals. SC-XRD results show that, the trapped perrhenate anions form multiple hydrogen bonds with the 3D framework in TJNU-244(Re) and TJNU-243(Re), and 2D layers of TJNU-334(Re) (Figures S15–S17). Nevertheless, only TJNU-244 follows the replacement mech-anism, while TJNU-243 and TJNU-334 undergo heavy lattice distortion.

As for TJNU-244(Re), it is monoclinic with a = 9.8123(4), b = 13.7736(6), c = 15.8082(7) Å, and β = 102.8010(10)°. The structure is similar to that of TJNU-244 before the anion exchange with the changes of the unit cell dimensions by –2%a, –5%b, +2%c and –2%β. The unit cell volume reduces by ca. 4% (Tables S1 and S2). And thus, it follows the *replacement* mechanism.

TJNU-243(Re) crystals are monoclinic with the unit cell parameters, a = 9.3392(3), b = 18.3221(3), c = 11.5364(4) Å, and β = 106.352(4)° (Part 2, Table S1). This unit cell is derived from that of the original TJNU-243 by changes of the parameters, –11%a, +26%b, –25%c, and –8.3%β. The unit cell volume changes by –9.8% (Tables S1 and S2). Such variation trends of TJNU-243(Re) are similar to those of TJNU-243(Cr), mainly because the strong interactions between ReO_4^- and Ag center (Ag···O = 2.825 Å), as well as multiple C–H···O (H···O bond length: 2.36–2.55 Å) bonds (Figure S16 and Table S4). Similarly, anion-exchange of perrhenate by TJNU-243 follows the *breath* mechanism, though no typical coordination bond between ReO_4^- and host framework is observed.

TJNU-334(Re) also has a monoclinic structure as determined by using SC-XRD with the unit cell parameters, a = 7.7040(11), b = 14.071(2), c = 16.550(2) Å, and β = 95.531(3)° (Part 3, Table S1). In comparison with TJNU-334, the significant changes of unit cell parameters are –55%a, +58%b, –9.2%c, and –3.8%β, and the unit cell volume contracts 35% (Tables S1 and S2). Interestingly, by carefully comparing the 2D structures of TJNU-334(Re) and TJNU-334, no coordination bond breakage was found. The tremendous structural changes in TJNU-334(Re) originate from the distortion of the 2D layers and shrinkage of the interlayer voids. Moreover, multiple C–H···O (H···O bond length: 2.37–2.58 Å) bonds were found between the perrhenate and 2D layers (Figure S17 and Table S4). As a result, this oxoanion-exchange can also be described as a *breath* process. Though in such *breath* processes, hydrogen bonding is weaker than coordination bonding, multiple localized hydrogen bonds can affect the sorption performances.

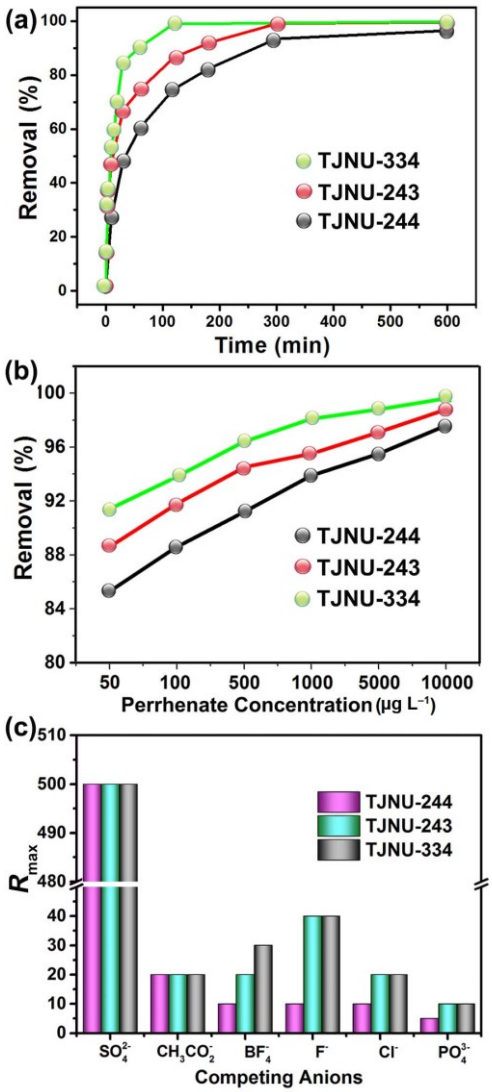

Figure 8. (a) Sorption isotherms for TJNU-CPs, showing the adsorption curves of perrhenate exchange capacities versus contact time in an aqueous solution. (b) Plots of perrhenate removal by TJNU-CPs in dilution solution from 50 μg L^{-1} to 10 mg L^{-1}. (c) The highest ratios of the competing anions to ReO_4^-, R_{max}, when the adsorption of the former was not detectable.

.

As expected, TJNU-243 and TJNU-334 show better sorption capability and selectivity than TJNU-244. Perrhenate removal results indicate that, the former two display higher removal capacities of 99.72% and 99.66%, respectively, than TJNU-244 (97.54%) (Figure 8a). The maximum adsorption capacities were measured to be 390, 472, and 455 mg of ReO_4^- per gram of TJNU-244, TJNU-243, and TJNU-334. The equilibrium adsorption time follows the order of TJNU-334 > TJNU-243 > TJNU-244. As for the very dilute solution of perrhenate, the removal efficiency follows the order of TJNU-334 > TJNU-243 > TJNU-244 (Figure 8b). Interestingly, all the TJNU-CPs(Re) display similar stabilities in aqueous solution of different pH values to their TJNU-CPs counterparts (Figure S18), which may be due to their similar coordination environments of Ag atom and absence of the vulnerable Ag–O(dichromate) bond. With regards to the thermal stability, the frameworks of TJNU-244(Re), TJNU-243(Re) and TJNU-334(Re) start to decompose upon 280, 221, and 315 °C, respectively (Figure S19).

As shown in Figures 8c and S20, TJNU-334 and TJNU-243 show higher selectivities than TJNU-244 towards most secondary anions (BF_4^-, F^-, Cl^-, and PO_4^{3-}), which can be attributed to the relatively stronger interactions between the framework of TJNU-243 or TJNU-334 and perrhenate anions. Because of the *replacement* and *breath* mechanisms of TJNU-CPs in perrhenate removal, all of TJNU-CPs possess good reversibility of over four cycles (Figures S21–S23). In particular, TJNU-243 and TJNU-334 display the interesting "breathing effect" during the reversible anion exchanges (Figure S24), due to their structure flexibilities.

Comparison in Adsorption of Dichromate and Perrhenate. As shown in Figures 6 and 8, the adsorption kinetics of each TJNU-CP sorbent towards dichromate and perrhenate is quite different. The equilibrium time of TJNU-CPs to adsorb dichromate is in the range of 8–30 hours, while the values for perrhenate removal are only 2–10 hours. In the oxoanion removal by TJNU-CPs, it follows the anti-Hofmeister bias,[30] which originates from their hydrophobic nature of channels constructed by pyridyl-rich organic ligands. Since dichromate has higher charge density than perrhenate, each TJNU-CP shows stronger affinity to perrhenate to result in faster adsorption kinetics.

As for the adsorption kinetics of three TJNU-CPs toward each anions, the trends of the equilibrium adsorption time are different, TJNU-243 > TJNU-334 > TJNU-244 for dichromate and TJNU-334 > TJNU-243 > TJNU-244 for perrhenate. The reasons may be hypothesized based on the distinct changes of single crystal structure. Firstly, dichromate and perrhenate removal by TJNU-244 are both following the *replacement* mechanism, in which no strong driving force exists to proceed the equilibrium. Thus, it shows the lowest adsorption kinetics. Secondly, in the dichromate removal by TJNU-243 and TJNU-334, TJNU-334 undergoes more complicated bond breakage and re-connection process and may require slightly longer time to achieve the adsorption equilibrium. Thirdly, with regards to the perrhenate adsorption by TJNU-243 and TJNU-334, no typical coordination bond between ReO_4^- and host framework was found in each anion-exchange product, TJNU-243(Re) and TJNU-334(Re). However, the 2D layers in TJNU-334(Re) allow a faster anion diffusion and show more flexibility to distort and shrink, providing a more favorable environment to fix perrhenate by multiple hydrogen bonds. It may promote the adsorption equilibrium.

CONCLUSION

In order to develop the methodology to integrate the outstanding oxoanion capture efficiency of chemisorption and remarkable recyclability into the same CP sorbent, three distinct anion-exchange mechanisms are proposed, such as *replacement*, *breath* and *reconstruction* processes, in accordance with different degrees of framework distortion in the CPs induced by the oxoanion adsorption. As expected, a superior sorbent should offer a *breath* process,[31] performing a strong chemisorption to ensure a high capture efficiency and the resulted framework distortion can be recovered during the reversed anion exchange. Herein, we have predicted and actually demonstrated that TJNU-243 is the best sorbent for dichromate removal via a *breath* process. Using the same CPs for removal of perrhenate from water, we identified TJNU-243 and TJNU-334 as excellent sorbents since both of them would work through a *breath* process. To achieve high level of both the properties, understanding the mechanism of the anion exchange and the microstructural evolution of the framework is essential. The established strategy in this work may shed light on research on removal of other oxoanions.

ASSOCIATED CONTENT

Supporting Information. The Supporting Information is available free of charge via the Internet at http://pubs.acs.org.
Detailed experimental and computation procedures, supplemental figures and schemes, and crystallographic parameters (PDF). X-ray crystallographic data of TJNU-CPs, TJNU-CPs(Cr), and TJNU-CPs(Re) (CIF).

AUTHOR INFORMATION

Corresponding Authors

*Email: hxxydm@tjnu.edu.cn; wzhou@st-andrews.ac.uk.

Present Address

School of Chemistry, University of St Andrews, St Andrews KY16 8SE, UK.

Notes

The authors declare no competing financial interest.

ACKNOWLEDGMENT

This work was financially supported by the National Natural Science Foundation of China (21571158 and 21771139), Tianjin Natural Science Foundation (17JCYBJC22800), and the Program for Innovative Research Team in University of Tianjin (TD13-5074).

REFERENCES

1 Sholl, D. S.; Lively, R. P. Seven chemical separations to change the world. *Nature* **2016**, *532,* 435–437.
2 Keith, L. H.; Telliard, W. A. ES&T special report: priority pollutants: I-a perspective view. *Environ. Sci. Technol.* **1979**, *13*, 416–423.
3 Katayev, E. A.; Kolesnikov, G. V.; Sessler, J. L. Molecular recognition of pertechnetate and perrhenate. *Chem. Soc. Rev.* **2009**, *38*, 1572–1586.
4 Sun, Q.; Zhu, L.; Augila, B.; Thallapally, P. K.; Xu, C.; Chen, J.; Wang, S.; Rogers, D.; Ma, S. Optimizing radionuclide sequestration in anion nanotraps with record pertechnetate sorption. *Nat. Commun.* **2019**, *10*, 1646.
5 Lim, J. Y. C.; Beer, P. D. Superior perrhenate anion recognition in water by a halogen bonding acyclic receptor. *Chem. Commun.* **2015**, *51*, 3686–3688.
6 Rapti, S.; Pournara, A.; Sarma, D.; Papadas, I. T.; Armatas, G. S.; Tsipis, A. C.; Lazarides, T.; Kanatzidis, M. G.; Manos, M. J. Selective capture of hexavalent chromium from an anion-exchange column of metal organic resin–alginic acid composite. *Chem. Sci.* **2016**, *7*, 2427–2436.
7 Oliver, S. R. J. Cationic inorganic materials for anionic pollutant trapping and catalysis. *Chem. Soc. Rev.* **2009**, *38*, 1868–1881.
8 Mark, R.; Findley, W. N. Thermal expansion instability and creep in amine-cured epoxy resins. *Polym. Eng. Sci.* **1978**, *18*, 6–15.
9 Slater, A. G.; Cooper, A. I. Function-led design of new porous materials. *Science* **2015**, *348,* aaa8075.
10 Cheng, Y. J.; Wang, R.; Wang, S.; Xi, X. J.; Ma, L. F.; Zang, S. Q. Encapsulating $[Mo_3S_{13}]^{2-}$ clusters in cationic covalent organic frameworks: enhancing stability and recyclability by converting a homogeneous photocatalyst to a heterogeneous photocatalyst. *Chem. Commun.* **2018**, *54*, 13563–13566.
11 Li, X.-Y.; Li, Y.-Z.; Yang, Y.; Hou, L.; Wang, Y.-Y.; Zhu, Z. H. Efficient light hydrocarbon separation and CO_2 capture and conversion in a stable MOF with oxalamide-decorated polar tubes. *Chem. Commun.* **2017**, *53*, 12970–12973.
12 Kawano, M.; Fujita, M. Direct observation of crystalline-state guest exchange in coordination networks. *Coord. Chem. Rev.* **2007**, *251*, 2592–2605.
13 Li, C. P.; Chen, J.; Liu, C. S.; Du, M. Dynamic structural transformations of coordination supramolecular systems upon exogenous stimulation. *Chem. Commun*. **2015**, *51*, 2768–2781.
14 Li, J.; Wang, X. X.; Zhao, G. X.; Chen, C. L.; Chai, Z. F.; Alsaedi, A.; Hayat, T.; Wang, X. K. Metal–organic framework-based materials: superior adsorbents for the capture of toxic and radioactive metal ions. *Chem. Soc. Rev.* **2018**, *47*, 2322–2356.
15 Fu, H. R.; Xu, Z. X.; Zhang, J. Water-stable metal–organic frameworks for fast and high dichromate trapping via single-crystal-to-single-crystal ion exchange. *Chem. Mater.* **2015**, *27*, 205–210.
16 Fei, H. H.; Bresler, M. R.; Oliver, S. R. J. A new paradigm for anion trapping in high capacity and selectivity: crystal-to-crystal transformation of cationic materials. *J. Am. Chem. Soc.* **2011**, *133*, 11110–11113.
17 Zou, Y.-H.; Liang, J.; He, C.; Huang, Y.-B.; Cao, R. A mesoporous cationic metal–organic framework with a high density of positive charge for enhanced removal of dichromate from water. *Dalton Trans.* **2019**, *48*, 6680–6684.
18 *Toxicological Profile for Chromium* (Public Health Service Agency for Toxic Substances and Diseases Registry, U.S. Department of Health and Human Services, Atlanta, GA, **2012**).
19 Attix, F. H. *Introduction to Radiological Physics and Radiation Dosimetry*; Wiley-VCH: Weinheim, Germany, **1986**.
20 Banerjee, D.; Elsaidi, S. K.; Aguila, B.; Li, B. Y.; Kim, D.; Schweiger, M. J.; Kruger, A. A.; Doonan, C. J.; Ma, S. Q.; Thallapally, P. K. Removal of pertechnetate-related oxyanions from solution using functionalized hierarchical porous frameworks. *Chem. Eur. J.* **2016**, *22*, 17581–17584.
21 Li, J.; Dai, X.; Zhu, L.; Xu, C.; Zhang, D.; Silver, M. A.; Li, P.; Chen, L.; Li, Y.; Zuo, D.; Zhang, H.; Xiao, C.; Chen, J.; Diwu, J.; Farha, O. K.; Albrecht-Schmitt, T. E.; Chai, Z.; Wang, S. $^{99}TcO_4^-$ remediation by a cationic polymeric network. *Nat. Commun.* **2018,** *9*, 3007.
22 Zhu, L.; Sheng, D. P.; Xu, C.; Dai, X.; Silver, M. A.; Li, J.; Li, P.; Wang, Y. X.; Wang, Y. L.; Chen, L. H.; Xiao, C. L.; Chen, J.; Zhou, R. H.; Zhang, C.; Farha, O. K.; Chai, Z. F.; Albrecht-Schmitt, T. E.; Wang, S. Identifying the recognition site for selective trapping of $^{99}TcO_4^-$ in a hydrolytically stable and radiation resistant cationic metal-organic framework. *J. Am. Chem. Soc.* **2017,** *139*, 14873–14876.
23 Li, C. P.; Ai, J. Y.; Zhou, H.; Chen, Q.; Yang, Y. J.; He, H. M.; Du, M. Ultra-highly selective trapping of perrhenate/pertechnetate by a flexible cationic coordination framework. *Chem. Commun.* **2019**, *55*, 1841–1844.
24 Klingele, M. H.; Brooker, S. From *N*-substituted thioamides to symmetrical and unsymmetrical 3,4,5-trisubstituted 4*H*-1,2,4-triazoles: synthesis and characterisation of new chelating ligands. *Eur. J. Org. Chem*. **2004**, 3422–3434.
25 Shao, Z.; Huang, C.; Wu, Q.; Zhao, Y.; Xu, W.; Liu, Y.; Dang, J.; Hou, H. Ion exchange collaborating coordination substitution: More efficient Cr(VI) removal performance of a water-stable Cu^{II}-MOF material. *J. Hazard. Mater.* **2019**, *387*, 120719.
26 Kresse, G.; Hafner, J. *Ab initio* molecular dynamics for liquid metals. *Phys. Rev. B* **1993**, *47*, 558–561.
27 Zhou, W. Z.; Jefferson, D. A.; Thomas, J. M. Defect fluorite structures containing Bi_2O_3: the system Bi_2O_3–Nb_2O_5. *Proc. Roy. Soc. Lond*. **1986**, *A406*, 173–182.
28 Zhou, W. Z.; Jefferson, D. A.; Thomas, J. M. A new structure type in the Bi_2O_3–Nb_2O_5 system. *J. Solid State Chem*. **1987**, *70*, 129–136.

29 Costa, M.; Klein, C. B. Toxicity and carcinogenicity of chromium compounds in humans. *Crit. Rev. Toxicol.* **2006**, *36*, 155–163.
30 Sheng, D.; Zhu, L.; Xu, C.; Xiao, C.; Wang, Y.; Wang, Y.; Chen, L.; Diwu, J.; Chen, J.; Chai, Z.; Albrecht-Schmitt, T. E.; Wang, S. Efficient and Selective Uptake of TcO_4^- by a Cationic Metal-Organic Framework Material with Open Ag^+ Sites. *Environ. Sci. Technol.* **2017**, *51*, 3471–3479.
31 Yu, C.; Shao, Z.; Hou, H. A functionalized metal–organic framework decorated with O^- groups showing excellent performance for lead(II) removal from aqueous solution. *Chem. Sci.* **2017**, *8*, 7611–7619.

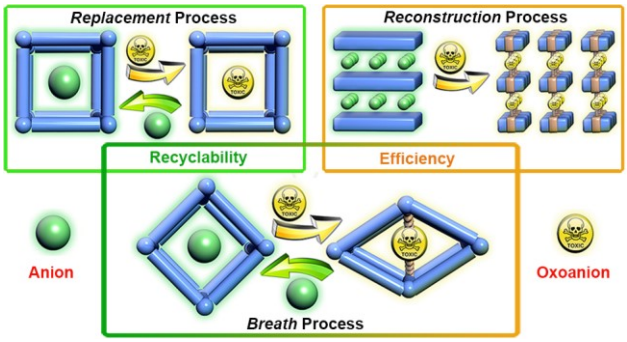
Replacement Process
Reconstruction Process
Recyclability
Efficiency
Anion
Oxoanion
Breath Process